

Recombinant Reflectin-Based Optical Materials

Guokui Qin,¹ Patrick B. Dennis,² Yuji Zhang,³ Xiao Hu,¹ Jason E. Bressner,¹ Zhongyuan Sun,¹ Wendy J. Crookes-Goodson,² Rajesh R. Naik,² Fiorenzo G. Omenetto,^{1,3} David L. Kaplan¹

¹Department of Biomedical Engineering, Tufts University, 4 Colby Street, Medford, Massachusetts 02155

²Air Force Research Laboratory, Materials and Manufacturing Directorate Biotechnology Group, Wright-Patterson Air Force Base, Dayton, Ohio 45433

³Department of Physics and Astronomy, Tufts University, 4 Colby Street, Medford, Massachusetts 02155

Correspondence to: D. L. Kaplan (E-mail: David.Kaplan@tufts.edu)

Received 7 October 2012; accepted 9 October 2012; published online

DOI: 10.1002/polb.23204

ABSTRACT: Reflectins are a unique group of structural proteins involved in dynamic optical systems in cephalopods that modulate incident light or bioluminescence. We describe cloning, structural characterization, and optical properties of a reflectin-based domain, refCBA, from reflectin 1a of Hawaiian bobtail squid, *Euprymna scolopes*. Thin films created from the recombinant protein refCBA display interesting optical features when the recombinant protein is appropriately organized. RefCBA was cloned and expressed as a soluble protein enabling purification, with little structural organization found using Fourier transform infrared spectroscopy and circular dichroism. Single-layer and multi-layer thin films of refCBA were then produced by flow coating and spin coating, and displayed colors

due to thin film interference. Diffraction experiments showed the assemblies were ordered enough to work as diffraction gratings to generate diffraction patterns. Nano-spheres and lamellar microstructures of refCBA samples were observed by scanning electron microscopy and atomic force microscopy. Despite the reduced complexity of the refCBA protein compared to natural reflectins, unique biomaterials with similar properties to reflectins were generated by self-assembled reflectin-based refCBA molecules. © 2012 Wiley Periodicals, Inc. *J Polym Sci Part B: Polym Phys* 000: 000–000, 2012

KEYWORDS: optics; reflectin; self-assembly; structural coloration; thin films

INTRODUCTION Natural optical features or coloration patterns are widespread across the animal kingdom, from the most exotic iridescent patterns of butterfly species to the feathers of peacocks and other birds.^{1–4} Camouflage and signaling/communication have emerged as two clear functions of structural coloration.^{3,5} Manipulation of light can be a significant selection pressure for the evolution of certain animal groups, leading to the diversity of natural photonic structures.³ Camouflage and communication signals can be created by reflecting daylight or by bioluminescence at night.^{5,6} For example, a Bragg reflector has high reflectance at a certain wavelength and low reflectance for other wavelengths. Structural color based on other structures was also investigated and mimicked.^{7–9} One of its natural analogs is the crystal multilayer structures of guanine, which are responsible for the colored reflection in many fishes.⁵ The helical arrangement of chitin microfibrils found in insects creates a periodicity that produces circularly polarized, colored reflection.⁵ These photonic structures are often found in the form of multilayer stacks of thin platelets in reflective tissues, resulting in refractive index differences between the alternating layers of platelets and spaces. This arrangement creates multi-layer interference that alters the reflection of light.

Varying the thickness between the alternating layers could offer further control over either the reflection coefficients or the spectral filtering.^{10,11}

Recently, a family of unusual proteins named reflectins has been found as the major component in flat, structural platelets in reflective tissues of the Hawaiian bobtail squid, *Euprymna scolopes* (Cephalopoda: Sepiolidae).¹⁰ It is believed that the specialized reflectin architectures produce structural color for camouflage and may contribute to the fields of materials science and optical nanotechnology.⁵ Recombinant reflectin proteins sequenced from the same species were expressed and purified in inclusion bodies with a molecular weight of 35–43 kDa.¹¹ These proteins exhibited diverse morphologies, unusual solubility, and self-organizing properties.¹¹ The proteins can be processed into thin films, diffraction grating structures, and fibers with potential applications in spectroscopic and optic fields.¹¹ This group of proteins was also found to be the material of the iridescence component in the dynamically responsive iridophores of the squid *Loligo pealeii*.¹² Further studies suggest that tyrosine phosphorylation of reflectin is involved in the regulation of dynamic iridescence in *L. pealeii*.¹² It has been recognized

Additional Supporting Information may be found in the online version of this article.

© 2012 Wiley Periodicals, Inc.

Report Documentation Page			Form Approved OMB No. 0704-0188		
Public reporting burden for the collection of information is estimated to average 1 hour per response, including the time for reviewing instructions, searching existing data sources, gathering and maintaining the data needed, and completing and reviewing the collection of information. Send comments regarding this burden estimate or any other aspect of this collection of information, including suggestions for reducing this burden, to Washington Headquarters Services, Directorate for Information Operations and Reports, 1215 Jefferson Davis Highway, Suite 1204, Arlington VA 22202-4302. Respondents should be aware that notwithstanding any other provision of law, no person shall be subject to a penalty for failing to comply with a collection of information if it does not display a currently valid OMB control number.					
1. REPORT DATE 2012		2. REPORT TYPE		3. DATES COVERED 00-00-2012 to 00-00-2012	
4. TITLE AND SUBTITLE Recombinant Reflectin-Based Optical Materials			5a. CONTRACT NUMBER		
			5b. GRANT NUMBER		
			5c. PROGRAM ELEMENT NUMBER		
6. AUTHOR(S)			5d. PROJECT NUMBER		
			5e. TASK NUMBER		
			5f. WORK UNIT NUMBER		
7. PERFORMING ORGANIZATION NAME(S) AND ADDRESS(ES) Air Force Research Laboratory, Materials and Manufacturing Directorate Biotechnology Group, Wright-Patterson Air Force Base, OH, 45433			8. PERFORMING ORGANIZATION REPORT NUMBER		
9. SPONSORING/MONITORING AGENCY NAME(S) AND ADDRESS(ES)			10. SPONSOR/MONITOR'S ACRONYM(S)		
			11. SPONSOR/MONITOR'S REPORT NUMBER(S)		
12. DISTRIBUTION/AVAILABILITY STATEMENT Approved for public release; distribution unlimited					
13. SUPPLEMENTARY NOTES JOURNAL OF POLYMER SCIENCE: PART B: POLYMER PHYSICS 2012, Government or Federal Purpose Rights License.					
14. ABSTRACT Reflectins are a unique group of structural proteins involved in dynamic optical systems in cephalopods that modulate incident light or bioluminescence. We describe cloning structural characterization, and optical properties of a reflectinbased domain, refCBA, from reflectin 1a of Hawaiian bobtail squid, Euprymna scolopes. Thin films created from the recombinant protein refCBA display interesting optical features when the recombinant protein is appropriately organized. RefCBA was cloned and expressed as a soluble protein enabling purification, with little structural organization found using Fourier transform infrared spectroscopy and circular dichroism. Single-layer and multi-layer thin films of refCBA were then produced by flow coating and spin coating, and displayed colors due to thin film interference. Diffraction experiments showed the assemblies were ordered enough to work as diffraction gratings to generate diffraction patterns. Nano-spheres and lamellar microstructures of refCBA samples were observed by scanning electron microscopy and atomic force microscopy. Despite the reduced complexity of the refCBA protein compared to natural reflectins, unique biomaterials with similar properties to reflectins were generated by self-assembled reflectin-based refCBA molecules.					
15. SUBJECT TERMS					
16. SECURITY CLASSIFICATION OF:			17. LIMITATION OF ABSTRACT Same as Report (SAR)	18. NUMBER OF PAGES 12	19a. NAME OF RESPONSIBLE PERSON
a. REPORT unclassified	b. ABSTRACT unclassified	c. THIS PAGE unclassified			

that supramolecular assembly of reflectin is a key property in the protein function.^{11,13} Previously, studies of native reflectin in the Loliginid squids demonstrated the responsive, tunable optical function of iridophore cells, and this dynamic optical function was facilitated by the hierarchical assembly of nanoscale protein particles that elicited large volume changes upon condensation.^{13,14} All of these data suggest that the proteinaceous nature of reflective tissues in squids may contribute their dynamic ability to modulate iridescent effects.

Reflectins are compositionally different from the reflective elements found in other marine and aquatic organisms, which are mostly composed of the purine crystals guanine and hypoxanthine.^{10,11} Proteins found in iridophores of the squid *L. pealeii* and RNA transcripts from the embryos of the cuttlefish *Sepia officinalis* have recently been shown to share homology with the reflectin family of proteins,¹⁵ suggesting that reflectin proteins may represent a ubiquitous, yet novel, optical nanostructural material among cephalopods.^{11,12} Analysis of reflectin sequences in *E. scolopes* revealed that reflectin proteins are encoded by at least six genes in three subfamilies and possess five repeating domains, which are well-conserved among members of the family. Each repeat contains a highly conserved core subdomain, defined by the repeating motif [M/FD(X)₅MD(X)₅MD(X)_{3/4}]. This subdomain is highly conserved among all reflectin proteins sequenced to date.^{10,15,16}

Here we further define subdomains of *E. scolopes* reflectin proteins and determine the self-assembly and optical properties of a recombinant form of *E. scolopes* reflectin 1a that contains a subset of these domains. Each repeat was previously divided into two subdomains based on a Rapid Detection and Alignment of Repeats alignment.¹⁰ The carboxyl-terminal half (A) consists of the highly conserved core subdomain, containing the repeating motif [M/FD(X)₅MD(X)₅MD(X)_{3/4}] (Supporting Information Figs. S1 and S2).¹⁰ The amino-terminal portion (B) of the repeat is less conserved among repeats, is enriched in tyrosine and asparagine residues, and is often terminated by a YPERY motif. Most reflectins also contain a domain between repeats 1 and 2 that is enriched in dityrosines, which we have termed the 'C' subdomain. Based on the sequence of reflectin 1a, we created a recombinant peptide refCBA, consisting of this intervening C domain (DYYGRFNDYDRYYGRSMF) and the B (NYGWMMDGDRYNRYNRWMDYPERY) and A subdomains of repeat 2 (MDMSGYQMDMSGRWMDMQGR).

To better understand the dynamic optical properties of squid reflectin, we characterized the properties and functions of this reflectin-based protein material refCBA, a block domain from native squid reflectin protein. To examine the fundamental relationships between reflectin chemistry, assembly, organization, and functional dynamic optical properties, we report the cloning of refCBA from reflectin protein in the Hawaiian bobtail squid *E. scolopes*. The observations of structure and coloration validate the role of this repeat motif in reflectin function. The studies suggest that reflectin-based

block domain refCBA is sufficient to confer the properties of full length reflectin, compared with previous studies on native reflectin proteins.¹³ The insights should facilitate further structural investigations into the functional properties of reflectin and shed light on more general aspects of the structure of reflectin proteins. We further discuss the significance of unique biomaterials with similar properties to reflectins, which can be used for spectroscopic and optical applications.

EXPERIMENTAL

Cloning, Expression, and Purification

Reflectin-based peptide sequences were constructed by annealing two synthetic nucleotides for each module as described previously.¹⁷ Reflectin block modules containing *NheI* and *SpeI* restriction sites were digested with these endonucleases and ligated into a pET30L vector that was previously digested, gel purified and dephosphorylated as shown in Supporting Information Figure S3. Ligation reactions were carried out using T4 DNA ligase (Invitrogen, Carlsbad, CA) at 16°C to generate a new plasmid for reflectin-based block domain refCBA. All expression vectors were transformed into *E. coli* RY-3041 strain, a mutant strain of *E. coli* BLR(DE3) defective in the expression of SlyD protein.¹⁸ Protein expression was induced with 1 mM IPTG (isopropyl β -D-thiogalactoside) (Fisher Scientific, Hampton, NH) and measured for several hours as reported previously.^{19,20} Protein purification was performed under native conditions on a Ni-NTA resin (Qiagen, Valencia, CA) using the manufacturer's guidelines. Further details and methods for gene and plasmid construction, protein expression and purification are available in the Supporting Information part. Protein purity and recovery rates were assessed by SDS-PAGE on 4–12% Bis-Tris precast gels (Invitrogen, CA). Protein identity was confirmed by N-terminal amino acid sequencing (Tufts Core Chemistry Facility, Boston, MA).

Physical Characterization

Structural characteristics of reflectin-based refCBA films were observed using Fourier transform infrared spectroscopy (FTIR) as previously reported.^{21–23} Spectra were scanned in absorption mode at 4 cm⁻¹ resolution from the 4000–400 cm⁻¹ region for 64 scans. The fractions of secondary structural components including random coil, alpha-helices, beta-strands and turns were evaluated using Fourier self-deconvolution (FSD) of the infrared absorbance spectra. FSD of the infrared spectra covering the amide I region (1595–1705 cm⁻¹) was performed by Opus 5.0 software. The average percent composition of the secondary structures was assessed by integrating the area of each deconvoluted curve and then normalizing this value to the total area of the amide I region. Circular dichroism (CD) spectra were also studied for the secondary structure of refCBA samples as previously described.^{20,24} All spectra were recorded at room temperature (25°C) using a 1 mm path-length quartz cell. RefCBA samples were measured in the Milli-Q water with concentrations of 0.5 mg/ml. CD data were analyzed using a DICHROWEB program (<http://dichroweb.cryst.bbk.ac.uk>).^{25,26} Absorbance

spectra with full-wavelength scanning for an aqueous protein solution of 0.5 mg/ml were characterized on an Aviv 14DS UV-Vis spectrophotometer equipped with a Peltier temperature controller (Aviv Biomedical, Lakewood, NJ). Fluorescence spectra of refCBA solution with excitation at 280 nm were collected using a Hitachi F4500 fluorescence spectrophotometer (Hitachi, Tokyo, Japan).

Sample Preparation and Thin Film Deposition

Flow Coating – Flow coating of recombinant refCBA from HFIP solutions was performed as reported previously.¹¹ RefCBA samples were freeze-dried in the lyophilizer and redissolved in HFIP. 50 μ l of 0.5% (w/v) refCBA/HFIP solution were injected under the blade of the flow-coating apparatus. The blade was carefully mounted so that the edge is 50 μ m above a silicon-wafer substrate (Wafer World Inc., FL, USA) and parallel to the wafer surface. The silicon-wafer substrate was directionally translated at constant velocity (10 mm s⁻¹) for 50 mm, spreading the protein solution to form a dry uniform thin film. We repeated this flow coating process on top of existing films to make multilayer films. Cross-flow coating was done by turning the direction of silicon-wafer substrate by approximately 90° and performing flow coating in the perpendicular direction. Using the same parameters in each run of the flow-coating process, including sample concentration, solution volume, blade height, blade angle, movement length, moving speed, thin films were generated with approximately the same thickness. Utilizing the same parameters in each run of the multiple flow-coating processes allow multi-layered films to be generated with total thicknesses 1X, 2X, 3X, 4X, 5X, 6X, etc.

Spin Coating – Reflectin-based samples were dissolved in the ultra-pure water with the different concentration, ranging from 1 to 5% (w/v). Then 100 μ l solutions were dispensed onto the polished silicon wafers (University Wafers, South Boston, MA) or cover slides (Fisher Scientific, Pittsburgh, PA). The silicon wafers had been previously cleaned by piranha solution (3:1 of sulfuric acid and 30% hydrogen peroxide, hazardous solution) for 1 h.¹³ Thin films were produced by spin coating the wafers in a WS-400E-6NPP/LITE spin processor (Laurell Technologies, North Wales, PA), operating at speeds between 500 and 1000 rpm for 30–60 s. After coating, the films were dried under a clean environment at the room temperature.

Morphology Observation and Microscopy

Optical Microscopy – Reflectin-based samples were freeze-dried to form thin layer structures, peeled off carefully and flat mounted on the glass slides. Images were taken with a hyperspectral CRi Nuance EX CCD camera (Woburn, MA) on an Olympus IX71 inverted microscope (Tokyo, Japan) under dark field. Spectral analysis of selected regions in the images was further performed, normalized, and smoothed using the CRi Nuance acquisition software (Woburn, MA).

Atomic Force Microscopy (AFM) – All imaging was performed in tapping mode on a Dimension 3100 Scanning Probe Microscope with Nanoscope V controllers (Digital Instruments, Santa Barbara, CA) and equipped with rotated

tapping-mode etched silicon probes (RTESP; Nanodevices, Santa Barbara, CA). Reflectin-based solution was cast on mica surfaces to form thin films. Images of the dried samples were captured at several random locations with surface areas ranging from 5 \times 5 μ m² to 0.5 \times 0.5 μ m². AFM observations were performed in air at room temperature using a 225 μ m long silicon cantilever with a spring constant of 3 N/m. Calibration of the cantilever tip-convolution effect was carried out to obtain the true dimensions of objects by previously reported methods.^{27,28}

Scanning Electron Microscopy (SEM) – SEM was used to assess additional morphological characterization of the freeze-dried protein samples. The experiments were performed using a Zeiss 55VP System (Oberkochen, Germany, at Harvard University Center for Nanoscale Systems, Cambridge, MA). Freeze-dried protein samples were first mounted on a silicon chip in a closed container at room temperature. SEM images were collected, after sputter coating (Cressington, 208HR) with a Pt/Pd target, using both InLens and secondary backscatter detectors.

Optical Studies and Spectral Measurements

Refractive Index (RI) – We casted thin films of refCBA sample with a thickness of a few μ m on the glass slides and measured the refractive index of the material films using a prism coupler (Metricon model 2010/M) with a 632.8 nm He-Ne laser (Different refractive indices may be observed by the light source with different wavelengths for same material). The refractive index was evaluated at 632.8 nm, and the RI and the thickness of the thin films were calculated based on the propagating modes with an accuracy of \pm 0.0005.

Thickness Evaluation – An Ocean Optics NanoCalc 2000 reflectometry system (Ocean Optics, Dunedin, FL) was used to analyze the thickness of thin films. Thin films of refCBA samples were first casted on the silicon wafers, and then the reflective spectrum of thin films was recorded in the spectrometer and their thicknesses were calculated based on thin film interference theory. The light source was the combination of a Deuterium lamp and a Halogen lamp, providing a wavelength range of 400–1100 nm. The resolution of the spectrometer was 1 nm.

Thickness Measurement – A Dektak 6M profiler (Veeco Instruments, Inc., Woodbury, NY) was used to measure the surface profile and thickness of the spin-coated thin films. Films were first scratched by a razor blade, and then the height difference between the film surface and the underlying substrate was measured along 5–10 nearby points in the region of the scratch as previously reported.²⁹

Relative Humidity (RH) – The spin-coated films on the silicon substrates were placed in a sealed plastic box. The RH was controlled using a Dydra electronic cigar humidifier and monitored using a Fisher Scientific temperature/RH meter (Fisher Scientific, Pittsburgh, PA).

Diffraction from Lyophilized RefCBA – A laser pen of 532 nm was used to illuminate lyophilized reflectin-based

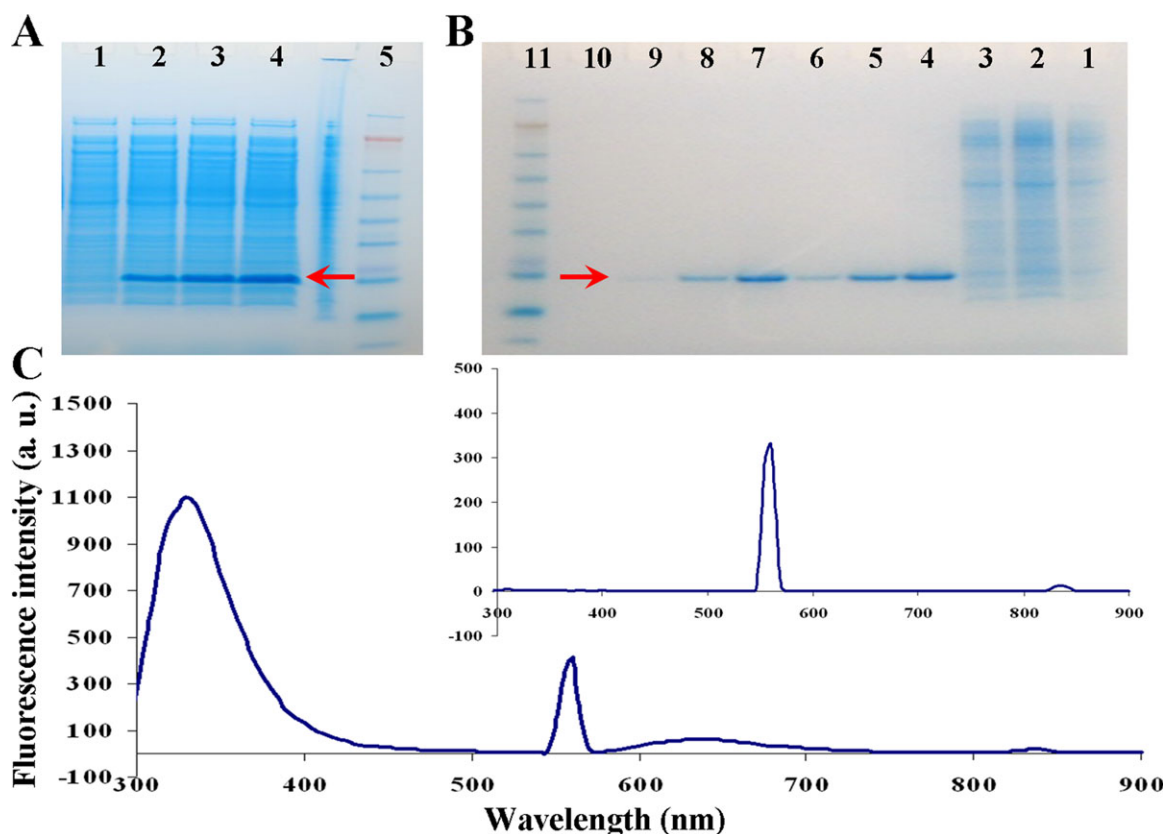


FIGURE 1 Protein expression, purification and fluorescence spectra of soluble refCBA. **A.** 4–12% SDS-PAGE of samples from expression. Lane 1–4, cleared supernatant from lysed cells expressed for 0, 2, 4, 6 h; Lane 5, see blue plus2 pre-stained standard (Invitrogen) was used as size markers (188, 98, 62, 49, 38, 28, 17, 14, 6, 3 kDa). **B.** 4–12% SDS-PAGE of samples from purification. Lane 1–2, flow through supernatant from lysed cells expressed for 6 h; Lane 3–6, collected fractions from Ni-NTA columns washed for four times by wash buffer; Lane 7–10, collected fractions from Ni-NTA columns washed for four times by elution buffer; Lane 11, see blue plus2 pre-stained standard (Invitrogen, Carlsbad, CA). **C.** Fluorescence emission spectra of refCBA. Fluorometric analysis indicated the maximum emission at 335 nm with the excitation at 280 nm. Inset is for the negative control of water.

samples that had ordered structures. The illumination beam was normal to the sample and diffraction pattern was observed on a white screen for analysis.

RESULTS

Design, Purification, and Determination

Our previously developed strategies for the biosynthesis of repetitive constructs¹⁸ was used for the reflectin-based block polymer, refCBA. After expression was carried out for 6 h at 30°C, the recombinant refCBA protein was purified as about 14 kDa [Fig. 1(A,B)]. Purity and identity of refCBA samples were confirmed by SDS-PAGE and N-terminal amino acid sequence analysis. In addition, the protein samples were observed as grey bands on the SDS-PAGE gels even without staining.¹⁰ The final purified yield of the reflectin-based protein was about 30 mg per liter of culture. The maximum absorbance around 275 nm was identified for reflectin-based refCBA samples, demonstrating typical protein characteristic of refCBA in Supporting Information Figure S4. Fluorometric analysis of reflectin-based refCBA indicated maximum emission at 335 nm with excitation at 280 nm [Fig. 1(C)], indicat-

ing a method to monitor the protein fractions by UV excitation.

Structural and Morphological Characterization

FTIR spectroscopy is useful for the study of the secondary structure of polypeptides and proteins. Lyophilized powders or dried films of the recombinant refCBA were examined by attenuated total reflectance (ATR) FTIR spectroscopy [Fig. 2(A)], which includes an expansion of the Amide I region for secondary structure analysis. The broad nature of the Amide I bands (centered around 1650 cm^{-1}) indicates the recombinant refCBA chains are mobile and sample a wide range of heterogeneous conformations. Peak deconvolution suggested potential contributions from all known secondary structures [Fig. 2(C)]. The band between 1635 and 1655 cm^{-1} (centered around 1650 cm^{-1}) exhibited characteristics of random coil configurations ($\sim 50\%$). This high degree of disorder is also consistent with the observed CD spectra [Fig. 2(B)]. These studies confirmed that the majority of the reflectin backbone exhibited random coil configurations, indicating that the overall the protein is dynamic and unstructured, with no likely transmembrane, alpha-helix or beta-sheet regions.

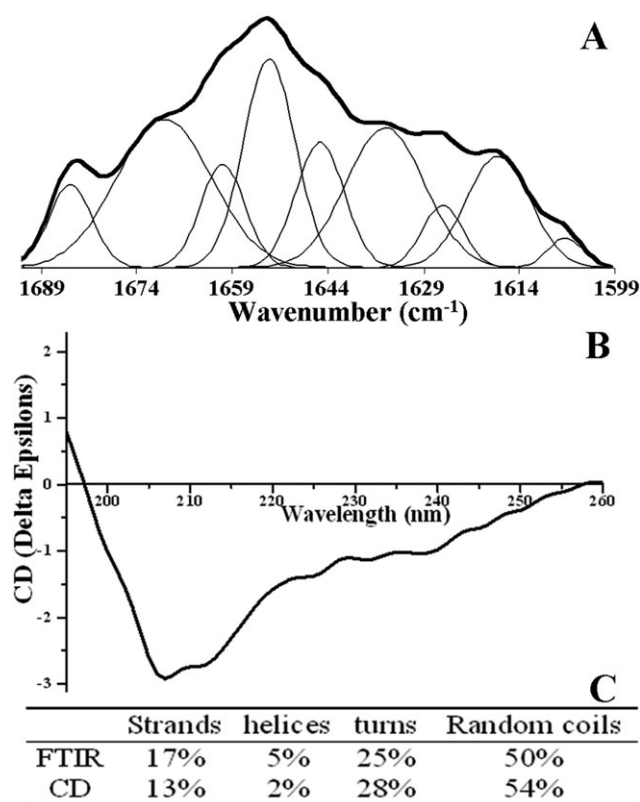


FIGURE 2 Secondary structure analysis of recombinant refCBA. **A.** Selected FTIR absorbance spectra of recombinant refCBA in the amide I' regions deduced after Fourier self-deconvolution. The heavy line represents the deduced absorbance band. The light lines represent the contributions to the amide I' band. **B.** Far-UV CD spectra. All spectra were recorded at room temperature (25°C) using a 1 mm path-length quartz cell with protein concentrations of 0.5 mg/ml. **C.** Secondary structure composition of reflectin-based refCBA by FTIR and CD.

The morphological characterization of freeze-dried reflectin-based materials was observed by a hyperspectral CRi Nuance EX CCD camera. Figure 3 presents images of the lamellar stacks obtained with lyophilized refCBA samples, indicating ordered parallel fibers structures with a period of around 15 μm connected with a very thin film. Each fiber shows a few different colors lines along its length. We examined the spectrum of these colors and found they have gradually shifting peak wavelengths [Fig. 3(C,D)], suggesting the refraction of white light source in the fiber.

Self-Assembly and Composition

To understand supramolecular assembly of reflectin-based samples, SEM was used to visualize the surface profile of self-organized recombinant refCBA. Similar lamellar structure of recombinant refCBA was observed as striped patterns with a uniform spacing of 10–15 μm [Fig. 4(A)]. These ordered structures were similar to diffraction gratings and were investigated for diffraction orders (See section “Fundamental Optical Properties”). Cross-sectional SEM images

were also obtained for reflectin-based refCBA films produced with higher concentrations up to 20 mg/ml as shown in Supporting Information Figure S5. We further deposited the refCBA solution with lower concentrations onto various substrates that were then air dried at room temperature, and then we employed a number of analytical tools for further characterization on the formed reflectin-based particles. AFM was used to observe surface morphologies and analyze the self-association of recombinant refCBA on to mica substrates. We observed the formation of nearly uniform protein nanoparticles with 20–30 nm in diameter when 0.5 mg/ml refCBA solution applied on to a mica substrate [Fig. 4(B)], suggesting the final aggregation of nanospheres that multimerize to form ordered structures as previously observed.¹¹

Thin Film Formation and Coloration

A flow-coating technique was used to generate thin films of recombinant refCBA. Similar concentrations and volumes were used for each run of flow-coating, allowing control of film thickness through multiple flow-coating steps. Thin films of 1–6 layers were prepared by repeated flow coating and films of 1–7 layers by cross flow coating. The same parameters for each run of the coating process were used, so each layer would be the same thickness. The thickness of each film increased proportionally as the layer number increased, as well as the colors of thin films ranging from the blue to the red end of the visible spectrum [Fig. 5(A)]. Furthermore, different samples showed repeatable color for thin films with same layer number. This result indicates colorimetric accuracy and repeatability to produce thin films with selected thicknesses and control the thickness of thin films by controlling the parameters of the multi flow-coating process, including amount and concentration of the solution, distance between the blade and the wafer surface, angle of the blade and translation speed.

To quantitatively demonstrate the relationship between reflected spectrum and thickness and test the coloration by thin film interference, we spin-coated single-layer thin films on the silicon-wafer substrate for reflectin-based proteins with different concentrations, ranging from 1 to 5%. Ideally the thickness of each spin-coated film was 1X, 2X, 3X, 4X, and 5X, respectively. The observed diffraction is shown in Figure 5(B). To study thin film interference theory for the single-layer reflectin films with different thicknesses, comparisons of reflectin-based materials was carried out between the simulated thickness calculated based on the reflective spectra and the real thickness measured by a Dektak 6M profiler. Normalized reflectance spectra were obtained with a visible wavelength range of 400–950 nm for reflectin-based thin films with different concentrations [Fig. 5(C)]. The thicknesses of different reflectin-based single-layer films of 1, 2, 3, 4, and 5% reflectin were then calculated to be 65, 106, 144, 156, and 200 nm, respectively, by the reflectometry system. Simulation based on thin film interference theory confirmed the calculations above (Supporting Information Fig. S6). These data agree well with the thicknesses physically measured by the profiler, which were 68, 99, 142, 146, and 212 nm, respectively. The slight difference between the

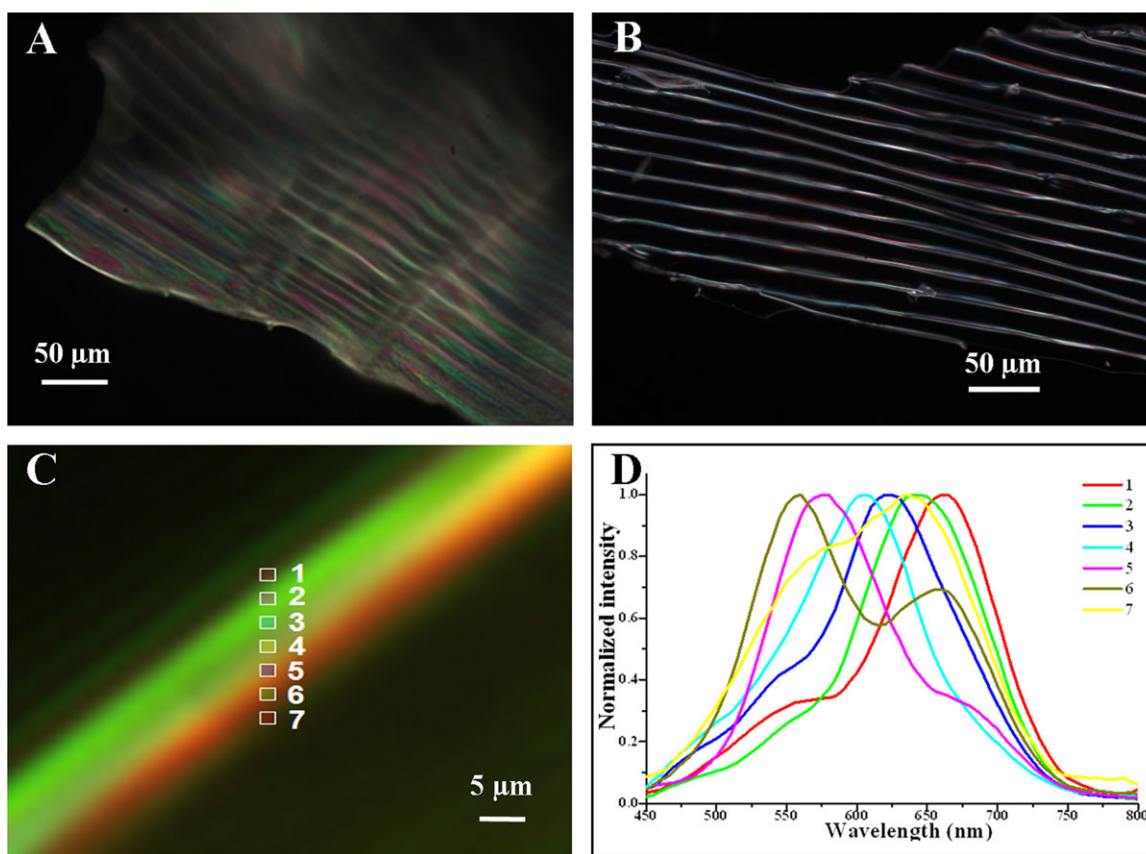


FIGURE 3 Morphological characterization and optical features of lyophilized recombinant refCBA using a hyperspectral CRI Nuance EX CCD camera on an Olympus IX71 inverted microscope under dark field (**A** & **B**). Spectral analysis of selected regions was further performed, normalized, and smoothed using the CRI Nuance acquisition software (**C** & **D**).

calculated and measured values can be explained by the uniformity of the film thickness. The thickness values were not close to ideal values 1X–5X, indicating nonrepeatable spin-coating. All of data above suggest the thin film interference theory provided a good explanation for color response to single-layer films with different thicknesses.

Previous studies reported the reflected spectrum of recombinant reflectin thin films was changed by dipping the sample in liquid.¹¹ Here we present more quantitative characterization of optical responses of reflectin-based thin films. Relative humidity (RH) may affect reflectin-based thin films through absorption or release of water vapor to make films thicker or thinner. If the films are thinner than $\sim 1 \mu\text{m}$, the color change can be observed by eye as the relative humidity changed. Previous studies indicated the reflected spectrum of recombinant reflectin thin film can be changed by dipping the sample in liquid.¹¹ Here we demonstrated the color change of reflectin-based thin films on silicon wafer was not visibly obvious when the relative humidity changed from 44 to 75%, but color change can be observed when the relative humidity was changed from 75 to 97% [Fig. 5(D)].

Fundamental Optical Properties

The refractive index of reflectin-based samples was found to be 1.5140 ± 0.0025 at 633 nm and 1.490 ± 0.0038 at 1300

nm [Fig. 6(A)]. Reflectin films of $\sim 2 \mu\text{m}$ thickness have a $>90\%$ transmission in the visible region (400–700 nm) whereas thicker films have lower transmission [Fig. 6(B)]. We observed ordered structures of self-assembled refCBA samples under optical microscope [Fig. 6(C)]. These structures were similar to the diffraction grating structure, and under the illumination of a laser pen (532 nm) were sufficiently order to generate diffraction spots [Fig. 6(D)]. Similar gratings were reported for full length reflectin.¹¹ According to the grating equation, the spacing of these diffraction orders agreed well with the period of the ordered structure observed under optical microscope. As an example shown in Figure 6(C,D), the spacing between the zeroth order and the first order was 2.2 cm and the distance between the sample and the screen was 46.3 cm. So the diffraction angle θ satisfies $\sin \theta = 2.2 / (2.2^2 + 46.3^2)^{1/2} = 0.0475$. According to the grating equation, $d \sin \theta = m\lambda$, when $\lambda = 532 \text{ nm}$ and $m = 1$, the corresponding grating period $d = 11.2 \mu\text{m}$. Examination under an optical microscope, the period of the ordered structure was found to be $11.1 \mu\text{m}$. The measured period agrees perfectly with the period calculated from the diffraction phenomenon. Furthermore, the orientation of the diffraction orders agrees reasonably with the orientation of the ordered structure if the refCBA sample was maintained the same direction both in the diffraction experiment and in the

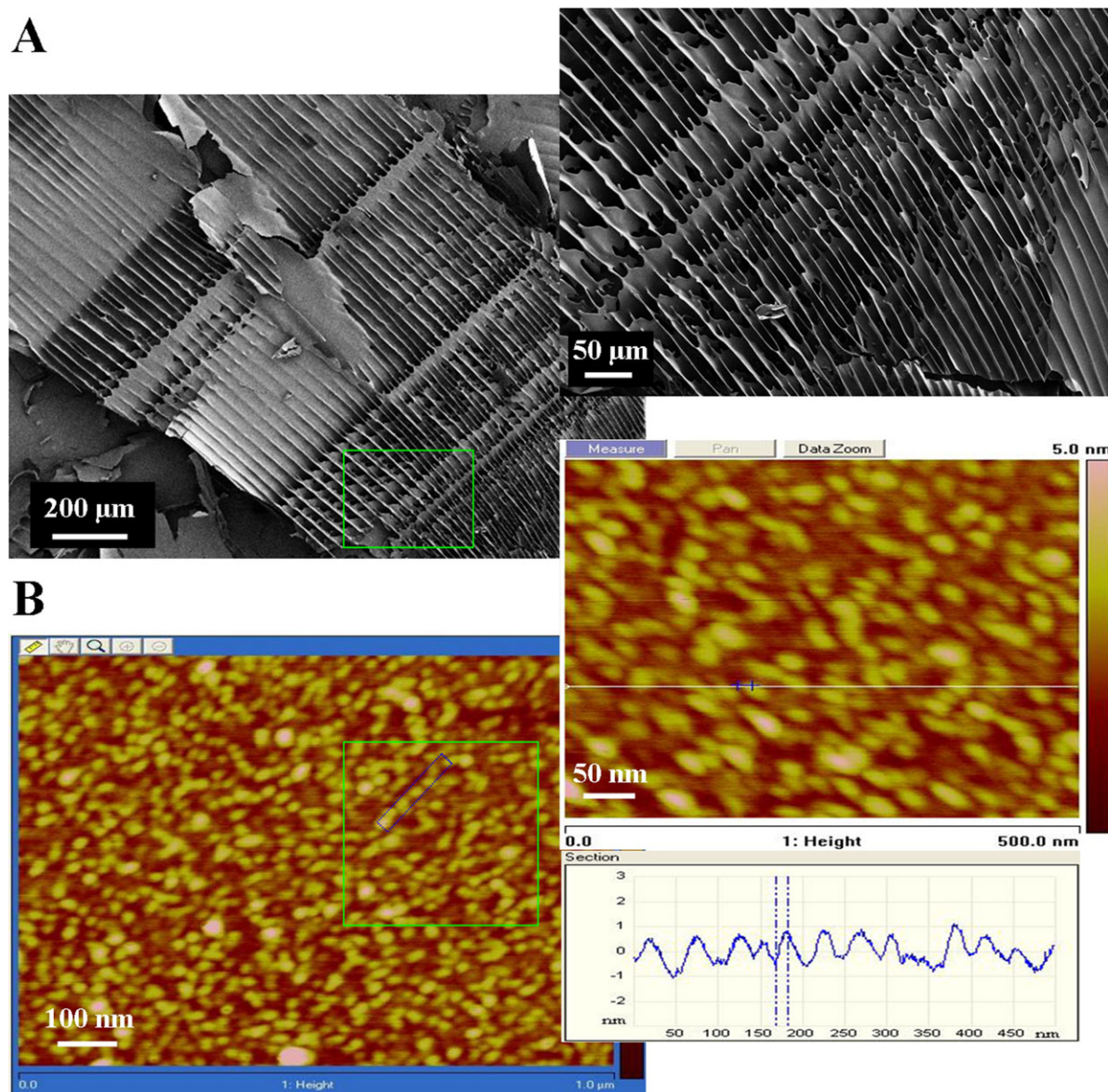


FIGURE 4 Self-assembly of lyophilized recombinant refCBA measured by SEM (A) and solution cast samples observed by AFM (B). Lamellar microstructures and nano-spheres have been manipulated by self assembling of reflectin molecules.

microscope observation, so the ordered structure in self-assembled refCBA is responsible for the diffraction pattern.

DISCUSSION

Cephalopods have received interest from materials scientists because of their hallmark camouflage abilities including the rapid change of the color and reflectance of their skin.¹³ Highly precise arrangements and orientations of reflectin proteins, the major biomaterial component of iridosomes in the bobtail squid, represent an example of natural nanofabrication of photonic structures.¹⁰ Early attempts at “bottom-up” synthesis to produce native reflectin proteins resulted in expression mainly in the form of inclusion bodies (approximately 35–40 kDa).^{11,13} In the present study, we cloned and expressed a water-soluble form of the reflectin-based protein

refCBA (approximately 14 kDa) containing a repeat domain from the *E. scolopes* squid. The refCBA protein was purified under native conditions on a Ni-NTA resin and allowed further characterization. Compared with native reflectin 1a from the same species,^{10,11} both the purified refCBA and native reflectins can be dissolved in 1,1,1,3,3,3 hexafluoroisopropanol (HFIP), the ionic liquid, 1-butyl-3-methylimidazolium chloride (BMIM), and SDS. SDS solubility suggested a character membrane-association, but no hydrophobic and trans-membrane domains are predicted based on the amino acid sequences. Membrane-cytoplasm interfaces are known to exhibit unique solubility properties relative to aqueous cytoplasm.

Native reflectin proteins were extracted from the multilayer reflector of the squid,^{10,12} and found to be insoluble with high methionine and arginine content. Polar aromatic

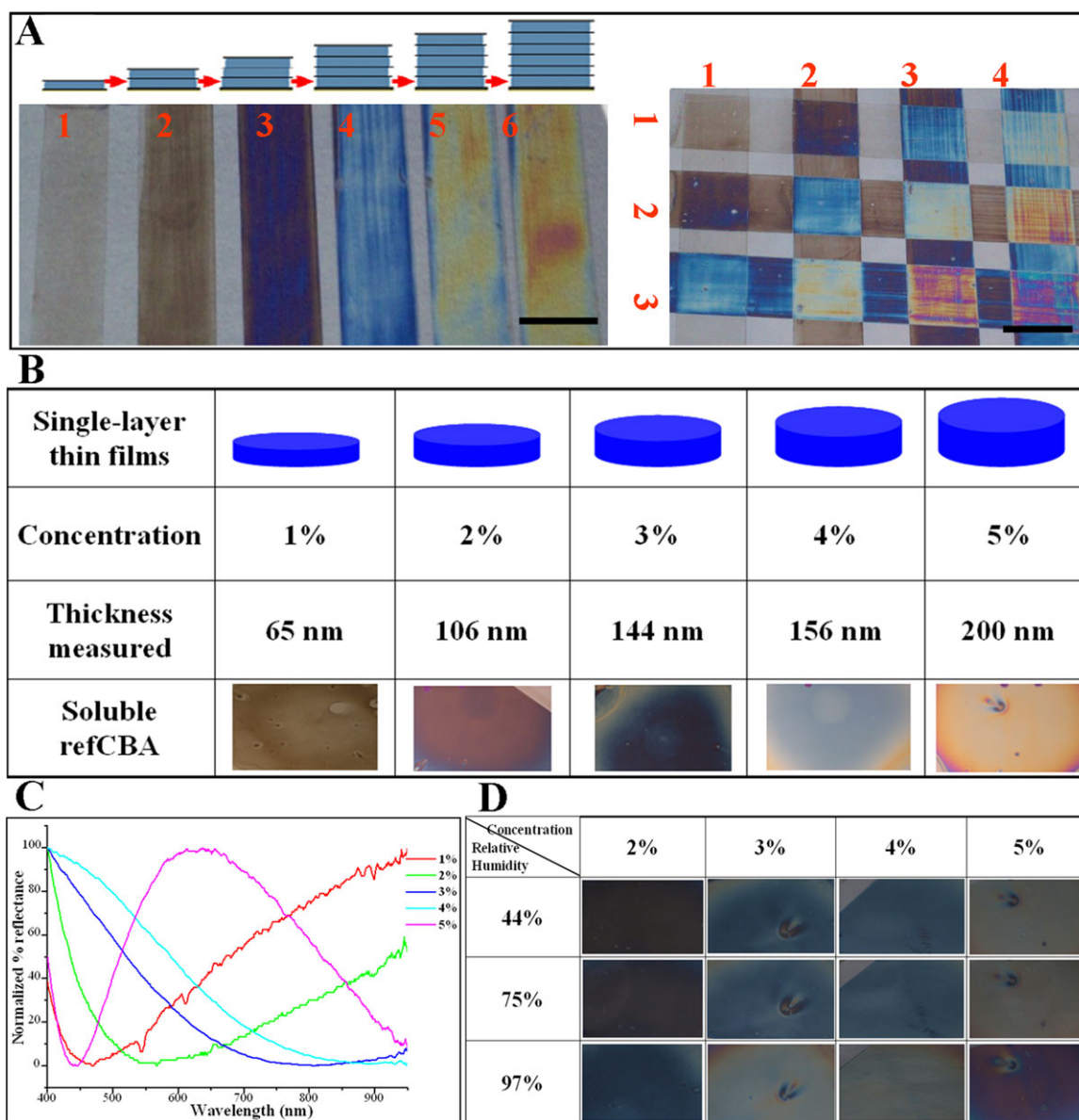


FIGURE 5 Thin film formation and structural coloration of reflectin-based materials. **A.** Solution casting of recombinant refCBA stacked thin films by flow (left) and cross-flow (right) coating techniques. Reflectin films exhibiting uniform thicknesses cast from a reflectin/HFIP solution. Scale bar is 1 cm. Number 1–6 indicates layer number. **B.** The single-layer thin films spin-coated for recombinant refCBA with a range of concentration from 1 to 5%. Different color responses present here for different samples as concentrations increased, as well as film thickness increased. **C.** Normalized reflectance spectra obtained with a visible wavelength range of 400–950 nm for reflectin-based thin films with different concentrations. **D.** Dynamic color response of spin-coated thin films with different concentrations as relative humidity changed. The color change of reflectin-based thin films on silicon wafer was not obviously visible when the relative humidity changed from 44 to 75%, but the color change can be observed obviously when the relative humidity changed from 75 to 97%.

residues are particularly stable in the membrane-interface regions, and arginine, because of its positive charge and long hydrophobic stem, exhibits ‘snorkeling’ behavior from the interface into the membrane.¹² Computational predictions revealed reflectins lack any distinct trans-membrane helices or hydrophobic regions. Our structure studies of reflectin-based proteins confirm that the majority of the recombinant refCBA backbone exhibited random coil configuration, indicating that the overall the protein was dynamic and unstruc-

tured, with no likely transmembrane, alpha-helix or beta-sheet regions.

Protein self-assembly into ordered arrays is generally considered critical for the function of structural proteins. In the present work we explored the biophysical and biophotonic properties of a reflectin-based domain refCBA, which is one of the repeating domains of native reflectins. The studies highlight the *in vitro* self-assembling properties by observing

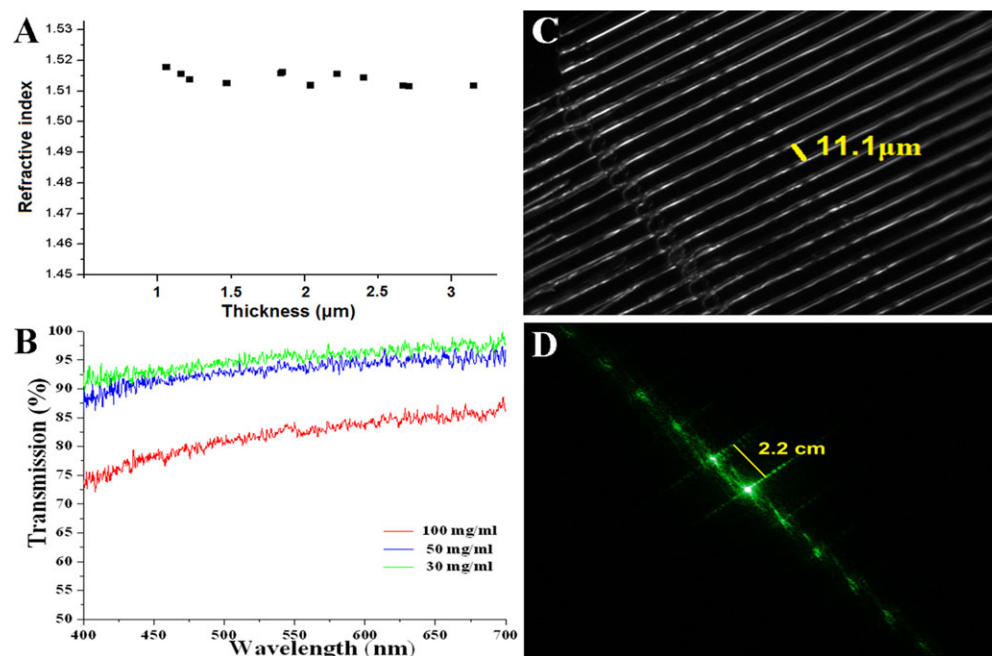


FIGURE 6 Optical properties and surface diffraction gratings produced from reflectin-based materials. **A.** Refractive index measurement of recombinant refCBA using a Metricon prism coupler. A refractive index of 1.5140 ± 0.0025 at 633 nm was observed, with no obvious changes as the film thickness increasing. **B.** Transmission Spectra of reflectin-based thin films. A $\sim 2 \mu\text{m}$ reflectin-based film has $> 90\%$ transmission in the region from 400 to 700 nm. Films with lower concentration will have better transmission, as the higher concentration of films will make films thicker. **C & D.** Surface diffraction gratings of reflectin-based patterned samples. 2.2 cm of the diffraction patterns was measured, corresponding to $11.1 \mu\text{m}$ of periodic spacing measured by an optical microscopy, as well as the micro-structure and orientation of reflectin-based patterned samples indicated.

the morphological characterization of recombinant refCBA. Complementary information can be obtained from the AFM images with regard to the individual domain morphologies. AFM images revealed that refCBA is hierarchically organized. At the nanoscale, the refCBA is composed of condensed assemblies of spherical protein particles from 20 to 30 nm in diameter as the nanospheres reported previously that assemble into fibrils.¹¹ The results demonstrate that these nanoparticles organize into morphologies, such as bead-on-a-string, connected networks, and close-packed assemblies.¹³ Significantly, we measure no evidence of secondary structure for refCBA by FTIR and CD, leading us to conclude that protein nanoparticles spontaneously assemble due to short-range interactions between extended strands. The self-association of refCBA is likely due to a combination of electrostatic and weak aromatic interactions because of the high content sulfur-containing and aromatic amino acids. These supramolecular architectures are simultaneously stabilized by alternating hydrophilic-hydrophobic portions of refCBA molecules. Our results with reflectin-based domain refCBA are consistent with previous studies on native reflectins.¹³ Aggregation of nanospheres will multimerize to form highly ordered structures, resulting in the progressive condensation of the reflectin nanoparticles into close-packed structures. The combination of self-assembly and processing can lead to the directed formation of lamellar structures, which were observable with optical microscopy and SEM studies. These

structures were ordered enough to generate diffraction orders. Ordered structures are the hallmark of multilayer reflectors,^{10,11} thus it is suggested that reflectin-based materials will transform and adapt structural requirements from natural organisms, due to the aggregation of an insoluble protein precursor into nanospheres that multimerize to form a well-organized structures.

Recent studies indicate cephalopods display an incredible ability to create eye-catching color by first using and modulating the highly ordered micro-structure of reflectin in 1D reflectors, known as iridophores, and then controlling absorption, reflection, and body surface texture. A variety of optical effects are involved, such as single-layer and multiple layer thin film interference, diffraction grating effects, photonic crystal effects, and scattering.²⁹ We believe the color change of the light reflected from these tunable reflectors is accomplished by either changing the thickness of the platelets themselves or the spacing between different refractive index platelets, suggesting a possibility to mimic this type of natural system by producing a single-layer or multiple layer biopolymer thin film with appropriate thickness. In addition, previous studies demonstrated the change in reflectin platelet thickness upon addition of acetylcholinesterase.³⁰

Initial attempts to create reflectin thin films for material properties and optical responses consisted of several different techniques prior to spin coating. First, various amounts of protein solution were drop casted onto different

substrates, such as silicon wafers, glass slides, mica and Teflon, resulting in inhomogeneous films. Other attempts to incorporate protein solution into the films during flow coating were successful,¹¹ although this technique sometimes negatively affected surface quality and structural coloration especially when applied for the formation of multilayer stack films. We also flow-coated multiple layers of reflectin-based thin films with different layers from 1 to 6 layers. The resulting films were annealed and cast on a silicon wafer for drying. The data indicated different color responses as the film layer or thickness was increased. To better understand the material properties of reflectin-based materials, we report the successful formation of smooth, reproducible thin films, using spin-coating deposition. Reflectin-based refCBA with different concentrations were spin-coated on silicon wafers to form different single-layer thin films with the corresponding color response, demonstrating the feasibility and repeatability of the spin-coating deposition.

Naturally occurring photonic materials in colorful insects and marine animals have been explored for new material design and protein-based nanofabrication in biomimetics.^{3,11} A change in protein platelet thickness can account for the observed optical response as iridophore color progresses from red to blue. In nature an iridescent iridophore within the squid mantle can reflect multiple colors, and post-translational modification of reflectin may dictate how these proteins change their aggregative state and the overall reflectance.¹² Biophysical and biophotonic properties of a highly reflective and self-organizing squid reflectin could lead to the development of nanofabrication photonic structures in the animal world. Because thin-film interference coatings give rise to multiple constructive and destructive interferences, reflectin films exhibit a dramatic spectral reflectance shift common to polymer-based thin films. All of the data from the short reflectin-based domain refCBA presented here have been shown the consistency with native reflectins from squids,¹¹ suggesting the potential of reflectin-based thin films as color-based biosensors. It would also be necessary to consider a number of physical factors such as mechanical strength, tensile, metal ion, and temperature and their effect on the corresponding color response.^{10,11} For example, the color response with the change of the reflective spectrum or thickness could be observed for stacked thin films of composite reflectin-based material system when tensile forces are applied.

The refractive index of recombinant reflectin-based refCBA was found to be 1.5140 ± 0.0025 at 633 nm, compared to 1.591 ± 0.002 at 589 nm for recombinant reflectin,¹¹ indicating a relatively high refractive index compared with other natural proteins. It has been known the photonic structures reflect light *in vivo* through alternating layers of high and low refractive index, suggesting new material designs with reflectin-based materials.^{1,31–34} Further investigation on increasing the selectivity and sensitivity of reflectin-based thin films might make optical-based detection more feasible. This may be achieved through the introduction of new biomaterials,^{19,20,35} addition of functional compounds, employ-

ing cross-linking strategies, or other chemical modifications. Additional studies include modes to bioengineer these chimeric reflectin-based systems with “triggers,” such that can be modulated to impact coloration patterns in a more dynamic way. In this way, the reflectin component will serve as the dynamic optical element. These approaches may include environmental or external stimuli, such as specific light pulses, enzymatic reactions, or relative humidity. The outcome of this effort would be a new family of dynamic optical materials with potential utility in a range of camouflage and related needs. Further analysis of reflectins should model the optical properties of these structures and inspire material synthesis with similar characteristics for various applications in optical nanotechnology.^{5,10,36,37}

CONCLUSIONS

A recombinant reflectin-based domain refCBA from squid reflectin protein was generated and characterized as a soluble protein. Our findings suggest this reflectin-based domain refCBA is sufficient to confer full length reflectin properties, compared with previous studies on native reflectin proteins. Lyophilized refCBA samples self-assembled to form ordered structures that were similar to diffraction gratings and were able to generate diffraction orders. Single- or multiple thin films by flow coating or via spin coating displayed repeatable reflectance properties, possessing a wide array of structural color due to thin film interference of reflected light. In many cases, physical and optical changes led to significant shifts in the reflected structural color. Here we report corresponding changes involved in film thickness for reflectin-based materials. Particularly notable are the large positive color response to the thickness associated with different concentration, lamellar stacks, and relative humidity.

ACKNOWLEDGEMENTS

Support from the AFOSR and the NIH (NIBIB, P41 EB002520) is gratefully acknowledged, as is support from DARPA.

REFERENCES AND NOTES

- 1 Shawkey, M. D.; Morehouse, N. I.; Vukusic, P. *J. R. Soc. Interface* **2009**, *6*, S221–231.
- 2 Zi, J.; Yu, X.; Li, Y.; Hu, X.; Xu, C.; Wang, X.; Liu, X.; Fu, R. *Proc. Natl. Acad. Sci. U S A* **2003**, *100*, 12576–12578.
- 3 Vukusic, P.; Sambles, J. R. *Nature* **2003**, *424*, 852–855.
- 4 Kinoshita, S.; Yoshioka, S. *Chemphyschem* **2005**, *6*, 1442–1459.
- 5 Mathger, L. M.; Denton, E. J.; Marshall, N. J.; Hanlon, R. T. *J. R. Soc. Interface* **2009**, *6*, S149–163.
- 6 Tong, D.; Rozas, N. S.; Oakley, T. H.; Mitchell, J.; Colley, N. J.; McFall-Ngai, M. J. *Proc. Natl. Acad. Sci. U S A* **2009**, *106*, 9836–9841.
- 7 Forster, J. D.; Noh, H.; Liew, S. F.; Saranathan, V.; Schreck, C. F.; Yang, L.; Park, J. G.; Prum, R. O.; Mochrie, S. G.; O’Hern, C. S.; Cao, H.; Dufresne, E. R. *Adv. Mater.* **2010**, *22*, 2939–2944.
- 8 Fudouzi, H.; Xia, Y. *Adv. Mater.* **2003**, *15*, 892–896.
- 9 Furutani, Y.; Ido, K.; Sasaki, M.; Ogawa, M.; Kandori, H. *Angew Chem. Int. Ed. Engl.* **2007**, *46*, 8010–8012.

- 10 Crookes, W. J.; Ding, L. L.; Huang, Q. L.; Kimbell, J. R.; Horwitz, J.; McFall-Ngai, M. J. *Science* **2004**, *303*, 235–238.
- 11 Kramer, R. M.; Crookes-Goodson, W. J.; Naik, R. R. *Nat. Mater.* **2007**, *6*, 533–538.
- 12 Izumi, M.; Sweeney, A. M.; Demartini, D.; Weaver, J. C.; Powers, M. L.; Tao, A.; Silvas, T. V.; Kramer, R. M.; Crookes-Goodson, W. J.; Mathger, L. M.; Naik, R. R.; Hanlon, R. T.; Morse, D. E. *J. R. Soc. Interface* **2010**, *7*, 549–560.
- 13 Tao, A. R.; DeMartini, D. G.; Izumi, M.; Sweeney, A. M.; Holt, A. L.; Morse, D. E. *Biomaterials* **2010**, *31*, 793–801.
- 14 Cooper, K. M.; Hanlon, R. T.; Budelmann, B. U. *Cell Tissue Res.* **1990**, *259*, 15–24.
- 15 Bassaglia, Y.; Bekel, T.; Da Silva, C.; Poulain, J.; Andouche, A.; Navet, S.; Bonnaud, L. *Gene* **2012**, *498*, 203–211.
- 16 Wardill, T. J.; Gonzalez-Bellido, P. T.; Crook, R. J.; Hanlon, R. T. *Proc. Biol. Sci.* **2012**, *279*, 4243–4252.
- 17 Rabotyagova, O. S.; Cebe, P.; Kaplan, D. L. *Biomacromolecules* **2009**, *10*, 229–236.
- 18 Bini, E.; Knight, D. P.; Kaplan, D. L. *J. Mol. Biol.* **2004**, *335*, 27–40.
- 19 Qin, G.; Rivkin, A.; Lapidot, S.; Hu, X.; Preis, I.; Arinus, S. B.; Dgany, O.; Shoseyov, O.; Kaplan, D. L. *Biomaterials* **2011**, *32*, 9231–9243.
- 20 Qin, G.; Lapidot, S.; Numata, K.; Hu, X.; Meirovitch, S.; Dekel, M.; Podoler, I.; Shoseyov, O.; Kaplan, D. L. *Biomacromolecules* **2009**, *10*, 3227–3234.
- 21 Hu, X.; Kaplan, D.; Cebe, P. *Macromolecules* **2006**, *39*, 6161–6170.
- 22 Hu, X.; Kaplan, D.; Cebe, P. *Macromolecules* **2008**, *41*, 3939–3948.
- 23 Qin, G.; Hu, X.; Cebe, P.; Kaplan, D. L. *Nat. Commun.* **2012**, *3*, 1003.
- 24 Greenfield, N. J. *Nat. Protoc.* **2006**, *1*, 2876–2890.
- 25 Whitmore, L.; Wallace, B. A. *Biopolymers* **2008**, *89*, 392–400.
- 26 Whitmore, L.; Wallace, B. A. *Nucleic Acids Res.* **2004**, *32*, W668–673.
- 27 Gomes, S.; Numata, K.; Leonor, I. B.; Mano, J. F.; Reis, R. L.; Kaplan, D. L. *Biomacromolecules* **2011**, *12*, 1675–1685.
- 28 Numata, K.; Cebe, P.; Kaplan, D. L. *Biomaterials* **2010**, *31*, 2926–2933.
- 29 Cathell, M. D.; Schauer, C. L. *Biomacromolecules* **2007**, *8*, 33–41.
- 30 Shashar, N.; Borst, D. T.; Ament, S. A.; Saidel, W. M.; Smolowitz, R. M.; Hanlon, R. T. *Biol. Bull.* **2001**, *201*, 267–268.
- 31 Shawkey, M. D.; Hill, G. E. *J. Exp. Biol.* **2006**, *209*, 1245–1250.
- 32 Omenetto, F. G.; Kaplan, D. L. *Science* **2010**, *329*, 528–531.
- 33 Amsden, J. J.; Domachuk, P.; Gopinath, A.; White, R. D.; Negro, L. D.; Kaplan, D. L.; Omenetto, F. G. *Adv. Mater.* **2010**, *22*, 1746–1749.
- 34 Lawrence, B. D.; Cronin-Golomb, M.; Georgakoudi, I.; Kaplan, D. L.; Omenetto, F. G. *Biomacromolecules* **2008**, *9*, 1214–1220.
- 35 Xia, X. X.; Xu, Q.; Hu, X.; Qin, G.; Kaplan, D. L. *Biomacromolecules* **2011**, *12*, 3844–3850.
- 36 Mathger, L. M.; Shashar, N.; Hanlon, R. T. *J. Exp. Biol.* **2009**, *212*, 2133–2140.
- 37 Yabu, H.; Nakanishi, T.; Hirai, Y.; Shimomura, M. *J. Mater. Chem.* **2011**, *21*, 15154–15156.